The onset of hazel wood formation in Norway spruce (Picea abies [L.] Karst.) stems

Vladimír Račko, František Kačík, Oľga Mišíková, Pavol Hlaváč, Igor Čunderlík, Jaroslav Ďurkovič

Annals of Forest Science (2018) 75: 82
https://doi.org/10.1007/s13595-018-0757-z

RESEARCH PAPER

The onset of hazel wood formation in Norway spruce (*Picea abies* [L.] Karst.) stems

Vladimír Račko[1] · František Kačík[2,3] · Oľga Mišíková[1] · Pavol Hlaváč[4] · Igor Čunderlík[1] · Jaroslav Ďurkovič[5]

Received: 23 February 2018 / Accepted: 9 July 2018 / Published online: 15 August 2018

Abstract

• ***Key message*** **Fungal infection was outlined as a potential reason for the onset of indented annual growth ring formation during the juvenile phase of hazel wood growth. Annual growth ring indentations resulted from the formation of disturbed zones which originated solely in close proximity to leaf traces.**

• ***Context*** Hazel wood is an abnormal type of woody tissue that is formed as a result of exogenous stimuli that may trigger long-term responses in the cambium. Cambial responses produce anatomical alterations in the surrounding xylem tissue that can be observed as an indentation of annual growth rings. The chemical profiles of lignan hydroxymatairesinol may provide an indication of its possible role in the protection of a living tree against the spread of a fungal or microbial infection at the onset of indentation.

• ***Aims*** The objectives of this study were to reveal the anatomical differences in the altered woody tissue of *Picea abies* hazel wood at both the onset and the later stages of annual growth ring indentation and to determine the chemical profiles for hydroxymatairesinol upon elicitation by a fungal infection in the disturbed zones.

• ***Methods*** Light and scanning electron microscopy observations were carried out on radial, tangential, and cross sections of hazel wood zones separated from *P. abies* stems. Concentrations of hydroxymatairesinol were determined for both the disturbed zones and the non-indented zones using a gradient high-performance liquid chromatography.

• ***Results*** The formation of disturbed zones was accompanied by significant changes in both the direction and width of the tracheids which produced an abnormal formation of intertwined and twisted tracheids. Fungal hyphae, radial cell wall cracks, and unusually large cross-field pitting were all found in the tracheids of the disturbed zones.

• ***Conclusion*** The content of hydroxymatairesinol in the acetone extract determined from the disturbed zones was 3.4 times greater than that present in the non-disturbed tissues. By means of vascular dysfunction in the leaf traces, host trees responded to the fungal infection by plugging the lumens of conductive leaf trace tissue and filling the vascular pathway with polyphenolic compound deposits.

Keywords Disturbed zone · Fungal infection · Hydroxymatairesinol · Indented annual growth ring · Leaf trace

Handling Editor: Jean-Michel Leban

Contribution of the co-authors All authors planned and designed the research. VR, FK, OM, PH, and IČ performed the experiments and JĎ analyzed the data. VR and JĎ wrote the manuscript. All authors reviewed and approved the manuscript.

✉ Jaroslav Ďurkovič
jaroslav.durkovic@tuzvo.sk

[1] Department of Wood Science, Technical University in Zvolen, 96053 Zvolen, Slovak Republic

[2] Department of Chemistry and Chemical Technologies, Technical University in Zvolen, 96053 Zvolen, Slovak Republic

[3] Department of Wood Processing, Czech University of Life Sciences in Prague, 16521 Prague 6, Czech Republic

[4] Department of Integrated Forest and Landscape Protection, Technical University in Zvolen, 96053 Zvolen, Slovak Republic

[5] Department of Phytology, Technical University in Zvolen, 960 53 Zvolen, Slovak Republic

1 Introduction

Figured wood describes certain well-defined patterns of wood found in many tree species. The patterns that occur over wide surfaces of lumber or veneer result from variations in the texture, grain, and color, as well as from the method of cutting (Beals and Davis 1977). One of the abnormal growth patterns of the annual growth ring is known as hazel growth or "Hasel wuchs" and was first described by Ziegler and Mertz (1961) in *Picea abies* wood. This growth pattern refers to a particular type of figured wood, also called "hazel wood" because of its close resemblance to the wood of various hazel species (genus *Corylus*) containing wide aggregate rays. For unknown reasons, certain regions of the annual growth rings exhibit reduced growth in the lenticular areas, and this growth pattern continues at the same location year after year. The result is the formation of lenticular depressions in the wood (Beals and Davis 1977). This phenomenon, referred to as an indentation of annual growth rings, describes local alterations in the annual growth ring shape induced by an anomalous dysfunction of the cambium. In cross sections of *P. abies* wood, annual growth rings are dipped towards the pith, whereas in radial sections, depending upon the reflection of light, the indentation invokes the impression of irregularly positioned wavy or curly zones of grains.

The figured hazel wood of *P. abies* may possess the resonance characteristics. Such wood displays remarkable acoustic properties compared to straight grain resonance wood and, thus, is frequently sought after for the manufacture of high-class violin soundboards (Bonamini et al. 1991; Buksnowitz et al. 2012). In the seventeenth century, this particular type of wood was also sought for making the most famous Italian violins. The indentation of annual growth rings not only modifies the elastic and acoustical anisotropy but also gives rise to the specific acoustical behavior of musical instruments made from such wood (Bonamini et al. 1991). High demand (both technical and commercial) for the valued hazel wood has prompted the development of a simple non-destructive method to identify annual growth ring indentations in living trees. This method enables the successful identification of bark indentations on a stem by splitting off small plaques of outer bark with a flat-nose screwdriver (Bonamini and Uzielli 1998).

Hazel wood formation can be found in many conifer species, such as *Picea abies* (Nocetti and Romagnoli 2008; Schultze and Gotze 1986; Ziegler and Mertz 1961), *Picea sitchensis* (Fukazawa and Ohtani 1984; Ohtani et al. 1987), *Pinus jeffreyi* (Ziegler and Mertz 1961), *Pinus halepensis* (Lev-Yadun and Aloni 1991), *Pinus taeda* (Tsoumis 1968), *Pseudotsuga menziesii* (Tsoumis 1968), *Cryptomeria japonica* (Imamura 1981), and *Cedrus libani* (Yaman 2007). Tracheids in the peripheral zones and occasionally in the central regions of the indented annual growth rings become distorted and twisted and tend to have varying lengths and widths. Shorter and wider tracheids are more frequently found in the indented juvenile annual growth rings than in the non-indented ones (Račko et al. 2016). Greater differences in tracheid dimensions between the indented and non-indented zones of hazel wood were found following a cambial zone injury (Lev-Yadun and Aloni 1991). Tracheids in marginal zones of the indented annual growth rings were observed to be distorted in a radial direction (Ziegler and Mertz 1961) and, simultaneously, slightly distorted tangentially (Ohtani et al. 1987). Furthermore, the occasional occurrence of a bordered pit was noted on the tangential cell walls of earlywood tracheids (Ohtani et al. 1987; Ziegler and Mertz 1961), as was the frequent occurrence of trabeculae (Grosser 1986; Ohtani et al. 1987). The rays present in the non-indented wood are mostly uniseriate and rarely biseriate, but the indented parts of annual growth rings show also multiseriate rays (Yaman 2007). An increase of approximately 40 to 50% was seen in the quantity of rays in the marginal disturbed zones of *P. abies* wood, and their volume showed an increase from 15 to 20% compared to the rays present in the non-indented regions. On the other hand, the average number of cells on the tangential section of a ray was diminished by some 10 to 20% (Ziegler and Mertz 1961). Anatomical features of altered hazel wood tissues are explained by abnormal cambial growth, but it is still unclear as to why or how they are produced (Nocetti and Romagnoli 2008). One of several possibilities is an injury that can induce their formation (Lev-Yadun and Aloni 1991). However, the question is why the induced changes persist for such a long period. In this context, the impact of other factors such as a fungal attack and environmental or genetic factors should also be considered. Notably, research in this area is still lacking.

The stem vascular system consists of a series of more or less distinct longitudinal strands that are organized in relation to the phyllotaxis of the shoot (Esau 1965). One or more stem vascular bundles (or, more usually, their branches) diverge into the base of each leaf (Nelson and Dengler 1997). These divergent thin vascular bundles are termed leaf traces which connect the vascular system of the stem with that of the leaf. As leaf traces are a conductive tissue, fungal or microbial pathogens may spread through this vascular pathway and potentially attack the internal tissues of the stem. Some lignans have potential antimicrobial, antifungal, antiviral, antioxidant, insecticidal, and antifeeding properties, and they probably play a notable role in plant defense against various biological pathogens and pests (Calvo-Flores et al. 2015). A new and exceptionally rich source of lignans are the knots of *P. abies* which contain on average about 10% by weight of lignans of which hydroxymatairesinol makes up 70–85% (Willför et al. 2003).

This study was aimed at both spatial and temporal anatomical assessments of the onset and the later stage development of the annual growth ring indentation in *P. abies* hazel wood, as well as at the determination of chemical profiles for lignan hydroxymatairesinol in the disturbed zones. We addressed the

following specific questions: (*i*) In which annual growth ring does the onset of indentations begin? (*ii*) Do or do not the disturbed zones originate from around the leaf traces, which are the conductive vascular pathway for the potential penetration of exogenous infections into the cambium and surrounding woody tissue? Potential reasons for the onset of indented annual growth ring formation in the juvenile phase of hazel wood growth are discussed.

2 Materials and methods

2.1 Plant material and sampling

Two felled *P. abies* trees, approximately 20 years of age with hazel wood zones, were obtained from a stand growing in the Muránska Planina National Park, Slovak Republic (48° 46′ N, 19° 59′ E, 1200 m a.s.l.). At the sawmill, during processing, the hazel wood zones were identified. Thus, the woody plant material, rather than being freshly felled and sampled from the trees, was approximately 1 week after felling. In addition, the stems had already been debarked prior to woody tissue sampling. For this reason, the anatomy of both the cambial layer and the bark could not be assessed during an examination of the indentation zones. The sample material that was used in the study is shown in Fig. 1a. Two debarked logs, having a diameter of 7.7 cm and a length of 1.2 m, were sliced into 51 wood disc pieces 2- to 5-cm thick. Subsequently, 51 wedge-shaped samples containing the entire hazel wood zones were separated from the discs. The wedge-shaped samples were split into 3 blocks, labeled B1–B3, each containing 5 indented annual growth rings (Fig. 1a). The B1 blocks were approximately 20 mm in length and 7 mm in the greatest width, the B2 blocks were approximately 12 mm in length and 10 mm in the greatest width, and the B3 blocks were approximately 10 mm in length and 11 mm in the greatest width. The inner B1 blocks, which contained the first (i.e., the most juvenile) 5 annual growth rings, were used for the anatomical assessment of early stages of indentation. The outer B2 and B3 blocks were used to assess a formation of indented annual growth rings in the later stages of the juvenile phase of development. The basic macroscopic characteristics of the plant material are presented in Table 1. More detailed information regarding both the tracheid morphology and the proportion of parenchyma cells within the indented zones was published in a recent study done by Račko et al. (2016).

2.2 Light microscopy

Wedge-shaped blocks were immersed in a deionized water for at least 120 min in order to soften the samples during sectioning. Transverse surfaces of the blocks were repeatedly covered with a starch-based non-Newtonian fluid (10 g cornstarch, 8 mL water, and 7 g glycerol) to avoid stripping off the secondary cell walls during sectioning (Schneider and Gärtner 2013). Radial, tangential, and cross sections, 15-μm thick, were cut with a sledge microtome (Reichert, Vienna, Austria) and transferred onto glass slides. After rinsing with water, the microsections were stained with 1% safranin and 1% astra blue (the staining solution was mixed in a ratio of 1:1) for at least 5 min. Thereafter, the microsections were rinsed with water, gradually dehydrated in ethanol (75 and 96%, respectively), and mounted in a drop of Euparal mounting medium beneath a coverslip according to standard protocol (Gričar et al. 2014). The slides were examined with an Axio Lab.A1 microscope (Carl Zeiss Microscopy, Jena, Germany).

2.3 Scanning electron microscopy

The excised leaf traces and surrounding disturbed zones were examined using scanning electron microscopy (SEM) for the presence of fungal infection. Radial sections, approximately 200-μm thick, were dried in a laboratory oven at 102 °C. The sections were mounted on specimen stubs, sputter-coated with gold using a Sputter Coater K650X vacuum chamber (Quorum Technologies, Ashford, UK) in an argon atmosphere with a gold layer thickness of 120 nm. Subsequently, the sections were placed in a desiccator to keep the moisture constant and observed by high-vacuum SEM using a VEGA TS 5130 instrument (Tescan Orsay Holding, Brno, Czech Republic) operating at 15 kV.

2.4 3-D reconstruction of the annual growth ring indentation

Two hazel wood zones were used to create a 3-D macro model of the annual growth ring indentation. Smooth transverse surfaces on the blocks were made with a sledge microtome (Reichert) and captured using a digital camera EOS 600D (Canon, Taichung Hsien, Taiwan). After each trim, the surface of the block was captured. Then, a series of images was created and converted to a stack of binary images using the image analysis software ImageJ to distinguish earlywood and latewood. A calibration of real dimensions for the hazel wood zone was carried out after the construction of the 3-D model.

2.5 Determination of selected extractives

Concentrations of hydroxymatairesinol and pinosylvin were determined in the samples separated from the first two annual growth rings for both the disturbed zones and the non-indented zones. The samples from both zones (approximately 80 mg of disintegrated wood each) were divided into two parts and extracted separately in a Soxhlet apparatus for 6 h with acetone and ethanol. Extracts were evaporated under a gentle stream of nitrogen. For high-performance liquid chromatography (HPLC), the samples were dissolved in methanol and filtered through Agilent

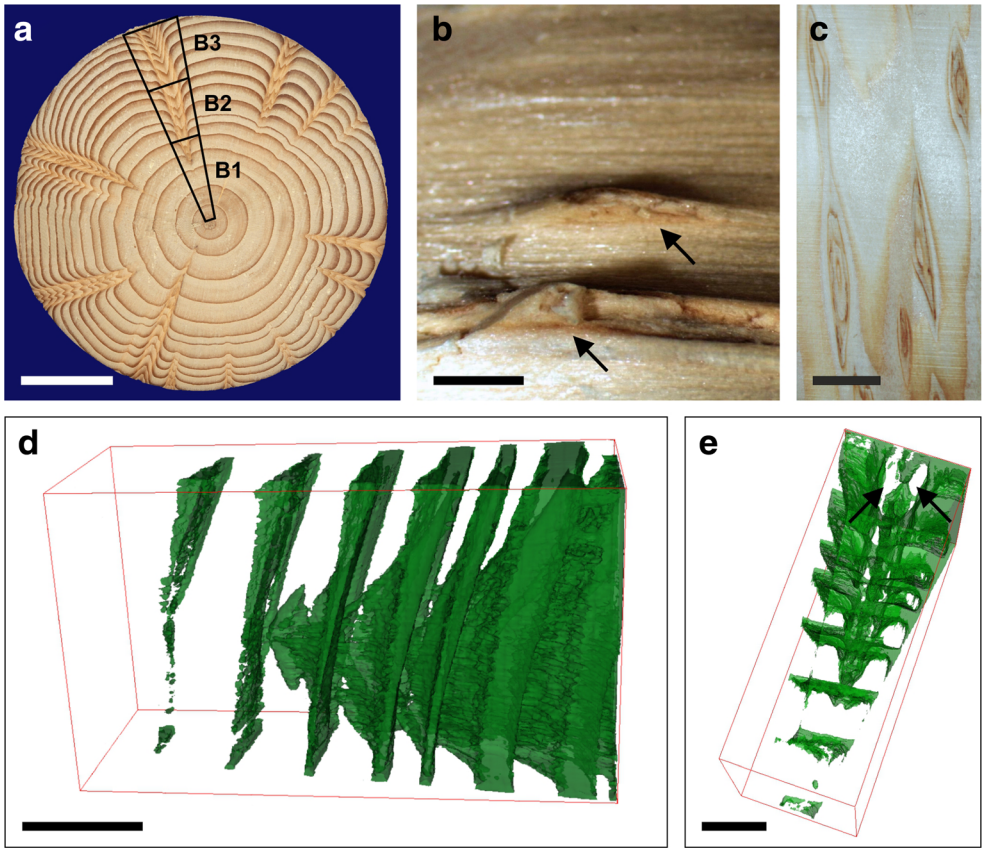

Fig. 1 Macroscopic characteristics of hazel wood zones. **a** Norway spruce stem disc containing the hazel wood zones, cross section. The wedge-shaped samples, labeled B1–B3, denote different blocks separated by age for microscopic observations. Cross section, scale bar = 2 cm. **b** Topographic profile of conical lenticular depressions within the fifth annual growth ring. The dark brown color is due to the presence of polyphenolic compounds (arrows). Tangential section, scale bar = 1 mm. **c** Various sizes of hazel wood zones coming from the tenth annual growth ring. Tangential section, scale bar = 1 cm. **d** The 3-D model of the shape and dimensions of the annual growth ring indentation which shows rapid changes in the early stages of indentation development. Scale bar = 1 cm. **e** In the 3-D model, the empty spaces at the margins of indented annual growth rings (arrows) denote the secondary disturbed zones which spread through several annual growth rings. Scale bar = 0.5 cm

Captiva Premium Syringe Filters (Agilent Technologies, Santa Clara, CA, USA) with a pore size of 0.45 μm. The gradient HPLC was carried out with an Agilent 1200 Series HPLC system (Agilent Technologies) equipped with a Kinetex C18, 2.6 μm, 100 × 4.6 mm column (Phenomenex, Torrance, CA, USA) at 35 °C. The mobile phase consisted of two solvents (A and B)

Table 1 Macroscopic characteristics of the non-indented wood and hazel wood zones

Trait	Annual growth rings class 1–5	Annual growth rings class 6–10	Annual growth ring class 11–15
Width of non-indented annual growth ring (mm)[1]	3.91 ± 0.21 a	2.48 ± 0.17 b	1.98 ± 0.14 c
Proportion of non-indented earlywood (%)[1]	86.63 ± 1.14 a	67.14 ± 5.76 b	59.02 ± 3.64 c
Proportion of non-indented latewood (%)[1]	13.37 ± 1.14 c	32.86 ± 5.76 b	40.98 ± 3.64 a
Height of hazel wood zone (mm)[2,3]	3.84 ± 1.87 c	16.59 ± 7.75 b	35.89 ± 11.53 a
Width of hazel wood zone (mm)[2,4]	1.19 ± 0.23 b	5.86 ± 1.15 a	6.10 ± 1.31 a

Data represent means ± SD. Mean values followed by the same letters, a–c across examined annual growth ring classes, are not significantly different at $P < 0.05$

[1] $n = 5$

[2] $n = 51$

[3] In longitudinal direction

[4] In tangential direction

and flowed with a programed gradient elution. The A solvent was methanol and the B solvent was a 0.1% phosphoric acid aqueous solution. Gradient program was as follows: 0 min, A/B = 40/60; 10 min, A/B = 40/60; 20 min, A/B = 90/10; 25 min, A/B = 40/60; 30 min, A/B = 40/60 (to equilibrate the column); and the flow rate was 1.0 mL min^{-1}.

2.6 Statistical analysis

The anatomical data comparing three annual growth ring classes (i.e., the first to the fifth, the sixth to the tenth, and the eleventh to the fifteenth annual growth ring class) were analyzed using a one-way analysis of variance and Duncan's multiple range tests to determine pairwise comparisons of means. The chemical data comparing the two types of woody tissues (i.e., disturbed and non-disturbed zones) were analyzed using Student's *t* test. As there was a significant variance difference between the examined woody tissues found for hydroxymatairesinol content in the ethanol extract, a *t* test for unequal variances was applied for this trait. In the remaining cases, variance differences between the woody tissues were non-significant, and *t* tests for equal variances were used.

Data availability The data and complementary microphotographs generated and/or analyzed during the current study are available from the corresponding author on reasonable request.

3 Results

3.1 Hazel wood zone characteristics

From the 51 examined hazel wood zones, 47 showed the onset of indentation in the second annual growth ring, and four other zones were identified in the third annual growth ring. In both cases, the onset of indentation was found in the midst of the growing season, approximately during the transition from earlywood to latewood. Conical lenticular depressions (Fig. 1b) within the annual growth rings were indented towards the pith, and on the tangential sections, they constituted spindle-like shapes (Fig. 1c). The greatest height of indentation was found in the eleventh to the fifteenth annual growth ring class (Table 1). The hazel wood zone width was least in the first to the fifth annual growth ring class. Then, it significantly increased in the sixth to the tenth annual growth ring class. However, a subsequent increase in the eleventh to the fifteenth annual growth ring class was negligible. The wider the annual growth ring, the deeper was the indentation (radially). The shape and dimensions of the conical lenticular depressions in the early stages of annual growth ring indentation may be clearly seen in Fig. 1d, e.

3.2 Formation of disturbed zones in the early stages of annual growth ring indentation

The macroscopically visible annual growth ring indentations resulted from the formation of disturbed zones which originated solely in close proximity to leaf traces (Fig. 2a–e). The formation of large disturbed zones was accompanied by significant changes in both the direction and width of the tracheids which produced an abnormal formation of intertwined and twisted tracheids (in all anatomical directions). Concurrently, the proportion of tracheids within the disturbed zones decreased. The occurrence of hypertrophy of parenchyma cells in the rays was observed to be rare during the earliest period of indentation development, but more frequent in the later period. In most cases, the disturbed zones were formed until about the end of the growing season within the second annual growth ring (Fig. 2a). Occasionally, the formation extended into the third annual growth ring (Fig. 2b). Later on, for unknown reasons, the formation of disturbed zones discontinued. The disturbed zones were not formed regularly around the entire perimeter of the leaf trace. Rather, they were formed on either side (Fig. 2c, e). The disturbed zones were frequently formed on the upper part of the leaf trace (Fig. 2a). But, sometimes, they were formed on the bottom part (Fig. 2b). The asymmetric position of disturbed zones affected the deflection of the surrounding tracheids in longitudinal and tangential directions. The slope of the tracheids was greater if they occurred near a large disturbed zone (Fig. 2a). The depth of indentation was dependent on the presence and robustness of the disturbed zone (Fig. 2c). In two cases, the disturbed zones were formed after the completion of the leaf trace formation (Fig. 2d). These two events resulted in a considerably greater deviation in the slope of tracheids and thereby in a deeper indentation of the following annual growth rings. Both radial (Fig. 2a, b) and transverse sections (Fig. 2c, d) showed that the conical lenticular depressions formed a deflection of the tracheid arrays which were arranged simultaneously in both longitudinal-radial and longitudinal-tangential directions. The disturbances of tracheids decreased with increasing distance from a leaf trace. Tracheids in undistorted marginal zones of indented annual growth rings were slightly undulated and intertwined (Fig. 2f). The deflection of tracheids was not changed, and the indentation also maintained its original shape behind the site where the leaf trace formation was completed in a radial direction. From both pathological and anatomical viewpoints, fungal hyphae, radial cell wall cracks, and unusually large cross-field pitting were all found in the tracheids of the disturbed zones in close proximity to leaf traces (Fig. 3a–d). By means of vascular dysfunction in the leaf traces, host trees responded to the fungal infection by plugging the lumens of conductive leaf trace tissue and filling the vascular pathway with polyphenolic compound deposits (Figs. 2a, 3e–f).

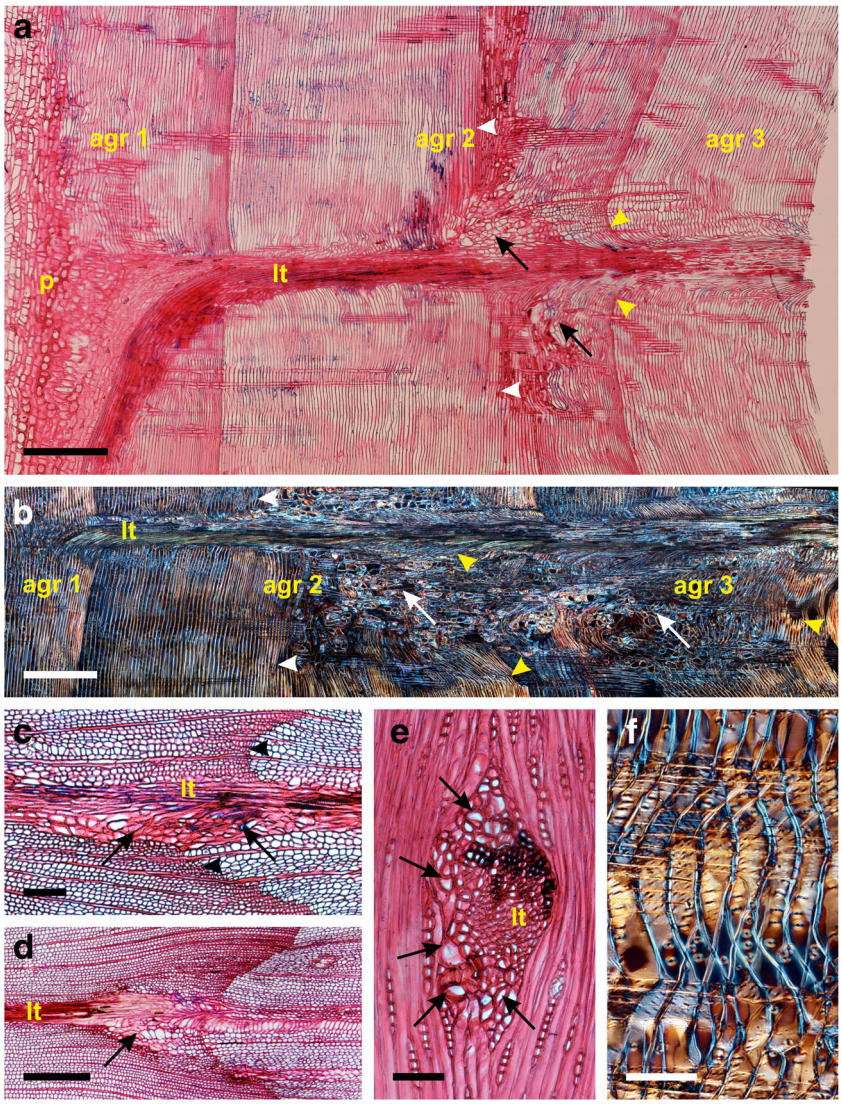

Fig. 2 The anatomy of indented annual growth ring tissues in the early stages of indentation. **a**, **b** Radial sections through the center of the leaf trace showing twisted tracheids in large disturbed zones (arrows) which induce the onset of indentation (white arrowheads) within annual growth ring. Yellow arrowheads show the reorientation of tracheids towards the cambium in a radial direction. The dark red color is due to the presence of polyphenolic compound deposits inside the leaf trace. **a** Bright-field and **b** polarized light microscopy, scale bars = 500 μm. **c** The effect of the asymmetry of the disturbed zone (arrows), associated with the leaf trace, on the depth of indentation within the annual growth ring (arrowheads). Cross section, scale bar = 200 μm. **d** The onset of indentation after the termination of the leaf trace formation. Cross section, scale bar = 500 μm. **e** The early stage of the disturbed zone formation (arrows) associated with the leaf trace growth. Tangential section, scale bar = 100 μm. **f** Intertwined tracheids in the marginal zone of indented annual growth ring. Radial section in polarized light microscopy, scale bar = 100 μm; agr, annual growth ring; lt, leaf trace; p, pith

3.3 Density of resin ducts and changes in the content of hydroxymatairesinol

The largest proportion of resin ducts per unit area of wood was found in the first two annual growth rings (Fig. 4). The resin ducts were primarily scattered in the latewood region of the annual growth ring. The occurrence of resin ducts in the earlywood region and at the boundary of the annual growth ring was quite rare. A proportion of the resin ducts remained unchanged in the disturbed zones or in close proximity to the site of indentation onset. Furthermore, typical rows of traumatic resin ducts were found neither in the early stages nor in the later period of indentation development.

Polyphenolic compounds, for the most part, were observed inside the lumens of the longitudinal tracheids and parenchyma ray cells (Fig. 5a–d) both of which occurred in close proximity to the disturbed zones. Wet chemical and HPLC analyses of the disturbed zones confirmed that yields of both the extractives and the amounts of lignan hydroxymatairesinol were significantly increased in these altered tissues (Table 2). The concentrations of hydroxymatairesinol extracted in acetone were higher than those extracted in ethanol. The content of hydroxymatairesinol in the acetone extract determined from the non-disturbed zones was on average 0.74%, whereas in the disturbed zones, it reached on average 2.50%, i.e., 3.4 times greater in content. Similarly, the content of hydroxymatairesinol in the ethanol extract determined from the disturbed zones was 2.6 times greater than that present in the non-disturbed tissues. However, the stilbenoid fungitoxin pinosylvin was not detected in either tissue.

3.4 Formation of secondary disturbed zones and their growth in later stages of annual growth ring indentation

Secondary disturbed zones were initiated in the marginal regions of the indented annual growth rings (Fig. 6a–d). These zones, characterized by their chaotic arrangement and at times

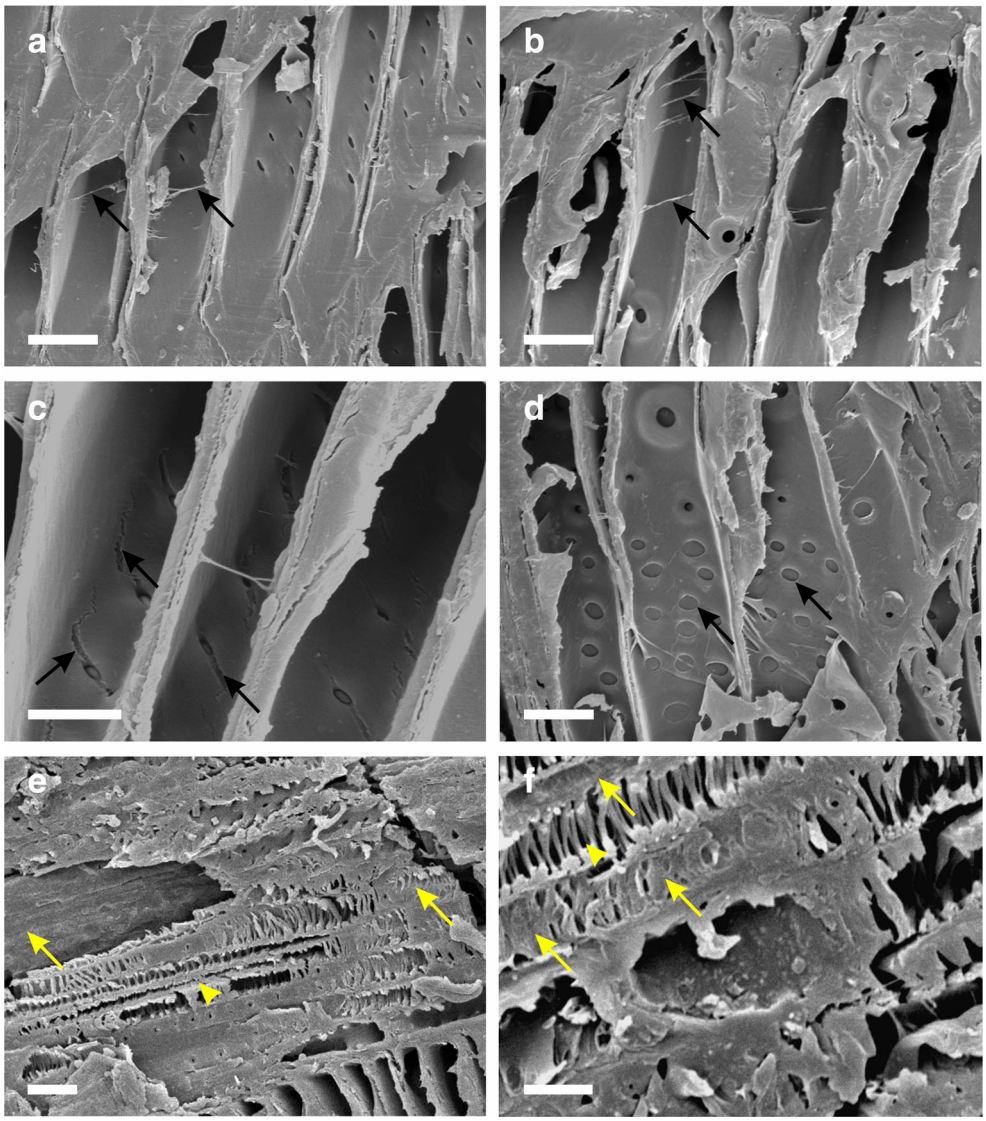

Fig. 3 Scanning electron microscopy images of fungal infection and anatomical abnormalities in primary disturbed zones. **a**, **b** Fungal hyphae present in tracheid lumens (arrows) in close proximity to the leaf trace. Radial sections, scale bars = 20 μm. **c** The onset of the tracheid cell wall degradation resulting in the formation of cell wall cracks (arrows). Radial section, scale bar = 10 μm. **d** Abnormally large cross-field pitting (arrows) at the intersections of longitudinal tracheids and ray parenchyma cells. Radial section, scale bar = 20 μm. **e**, **f** Leaf trace conductive tissue (arrowhead) which is plugged and filled with polyphenolic compound deposits (arrows). Radial sections, scale bar for **a** 20 μm; scale bar for **b** 10 μm

containing hypertrophied cellular elements, were formed by the cambium following termination of the primary disturbed zone formation responsible for the onset of hazel wood formation. Secondary disturbed zones, however, were not present in all hazel wood zones. The occurrence of secondary disturbed zones impacted the formation of new (secondary) indentations within the annual growth ring that has been previously indented (Fig. 6b). There was a considerable disturbance in the morphology of tracheids (Fig. 6c). The rays continuously increased their dimensions in a radial direction, especially within the secondary disturbed zones. The parenchyma cells of the rays changed their shape and dimensions, especially at the boundary of annual growth rings (Fig. 6e, f). These rays often aggregate to form either biseriate or multiseriate rays (Fig. 6e). Later, some of these rays split to become uniseriate (the onset of branching). During the later period of indentation, massive, heterogeneous, and multiseriate ray structures were formed, increasingly encroaching into the central regions of indented annual growth rings (Fig. 6g, h).

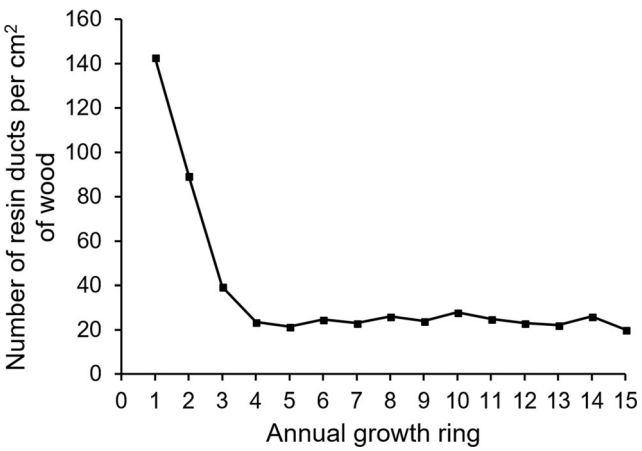

Fig. 4 Distribution of resin ducts per unit area of wood within annual growth rings

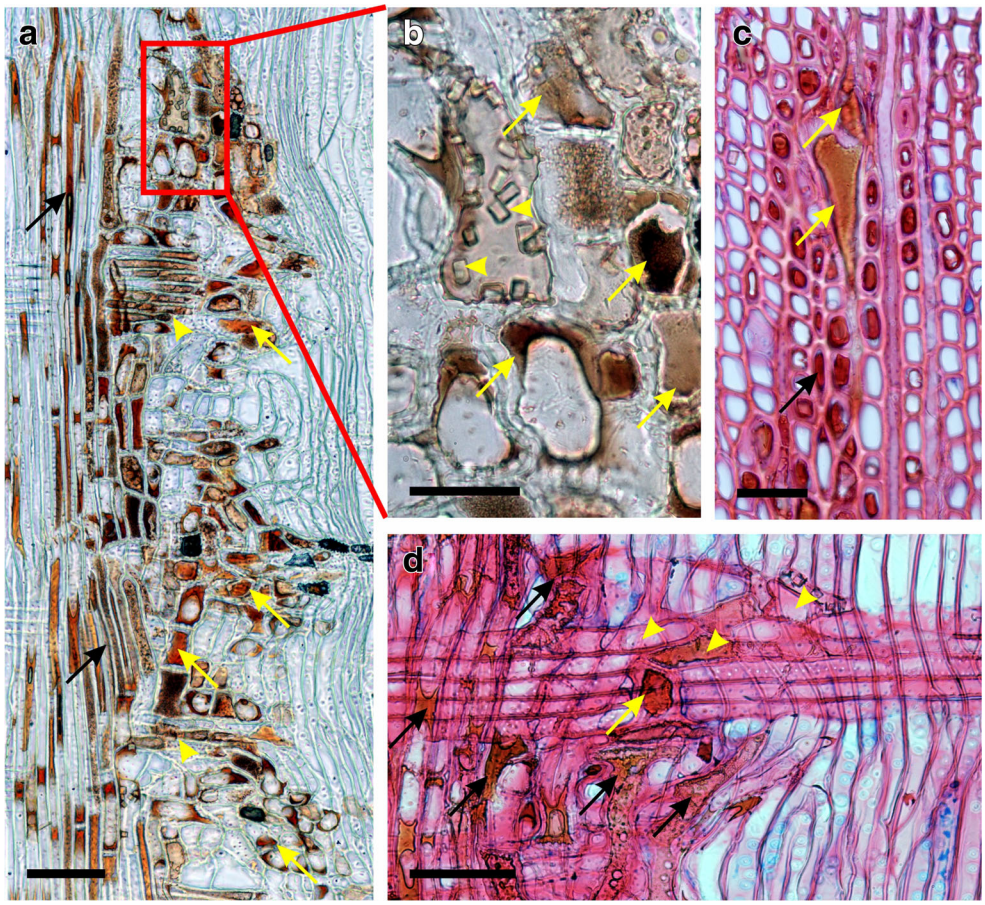

Fig. 5 Distribution of polyphenolic compounds within disturbed zones. **a** Polyphenolic compounds present inside the longitudinal tracheids (black arrows), parenchyma rays (arrowheads), and both disturbed tracheids and traumatic parenchyma cells (yellow arrows). Unstained radial section, scale bar = 100 μm. **b** Close-up view of disturbed cell lumens filled with polyphenolic compounds (arrows). Crystals were also present inside the traumatic parenchyma cells (arrowheads). Unstained radial section, scale bar = 50 μm. **c** Polyphenolic compounds inside undisturbed tracheid lumens (black arrow). Yellow arrows show residues of disturbed tracheids. Bright-field microscopy of the cross section made above a disturbed zone, scale bar = 50 μm. **d** Polyphenolic compounds inside disturbed tracheids (black arrows) located in close proximity to a parenchyma ray. Yellow arrow shows a large disturbed tracheid which disrupts the entirety of a ray. There was a conspicuous hypertrophy and disordering of parenchyma cells in the upper part of a ray (yellow arrowheads). Radial section, scale bar = 100 μm

4 Discussion

In this study, the early anatomical alterations of xylem tissues were observed exclusively in close proximity to the leaf trace structures. The chaotic entanglement of tracheids, the increase in their widths, and the decrease in their numbers suggest that the presence of exogenous stimuli triggered the formation of malformed tracheids. It has been reported that indentations are not due to differences in the timing of cell division or maturation (Nocetti and Romagnoli 2008). Our results indicated

Table 2 The content of hydroxymatairesinol and pinosylvin (% of oven dry weight) in the disturbed zones during the early stages of annual growth ring indentation ($n = 4$)

Extractives	Disturbed zone	Non-disturbed zone	*t* test (*P* value)
Yields of acetone extract	4.06 ± 0.03	1.98 ± 0.03	73.54 (0.0002) ***
Hydroxymatairesinol (in acetone extract)	2.50 ± 0.13	0.74 ± 0.06	23.91 (0.0001) ***
Yields of ethanol extract	1.36 ± 0.04	0.94 ± 0.04	9.90 (0.0101) *
Hydroxymatairesinol (in ethanol extract)	0.44 ± 0.02	0.17 ± 0.00	21.24 (0.0001) ***
Pinosylvin (in acetone extract)	ND	ND	NA
Pinosylvin (in ethanol extract)	ND	ND	NA

Data represent means ± SD. Significance denoted as ***$P < 0.001$ and *$P < 0.05$, respectively

ND, not detected; *NA*, not applied

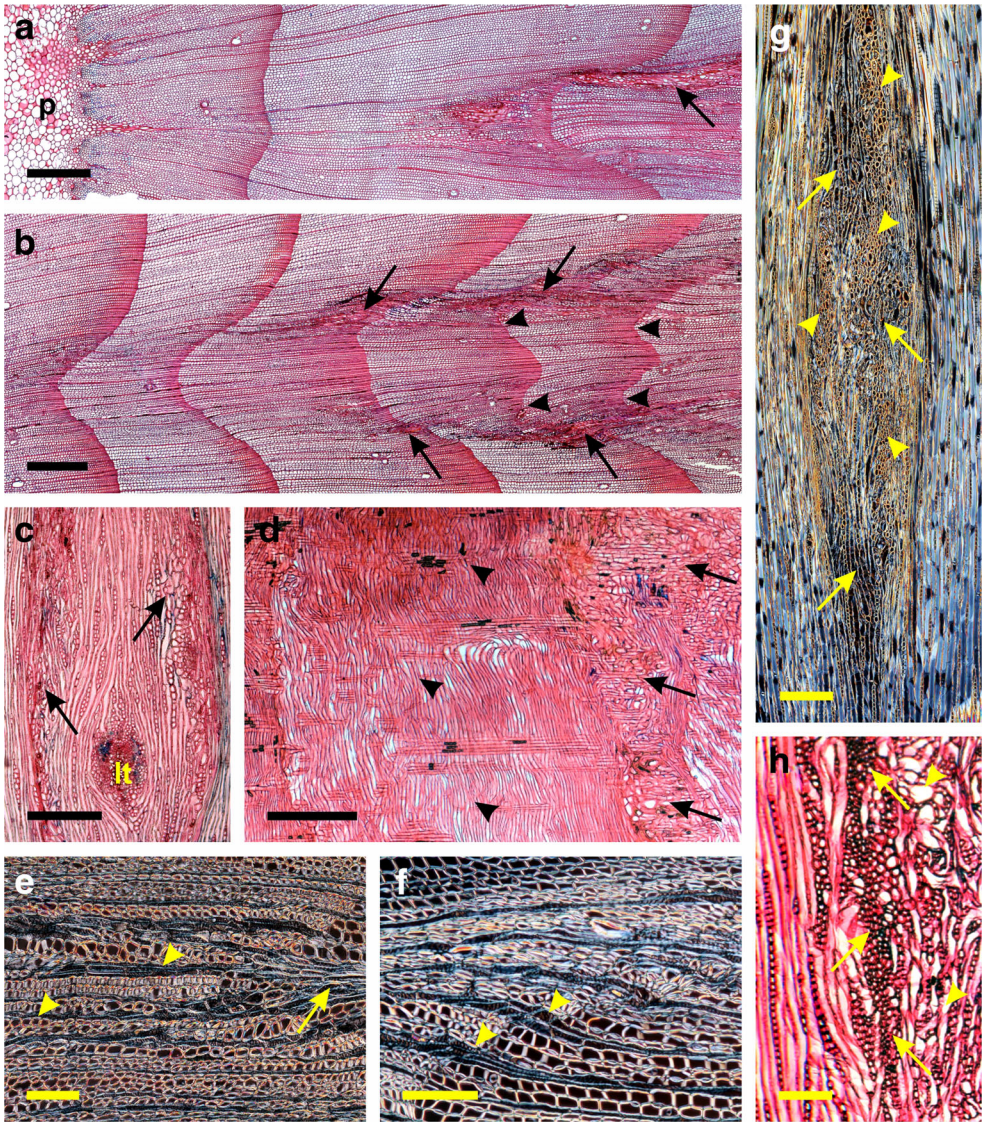

Fig. 6 The anatomy of secondary disturbed zones and their growth in the later stages of indentation. **a** Asymmetric formation of a secondary disturbed zone (arrow) after the termination of the primary disturbed zone formation in the third annual growth ring. Cross section, scale bar = 500 μm. **b** Symmetric formation of a secondary disturbed zone (arrows) in the third annual growth ring. Arrowheads show succeeding indentations within annual growth rings that have been previously indented. Cross section, scale bar = 500 μm. **c** Early stages of the formation of a secondary disturbed zone in the marginal zones of the fourth annual growth ring. Polyphenolic compounds present in both tracheids and parenchyma cells (arrows) while the leaf trace (lt) growth has not yet been completed. Tangential section, scale bar = 200 μm. **d** Secondary disturbed zone with rays and intertwined and twisted tracheids (arrows). Outside the zone, tracheids were only slightly undulated (arrowheads). Radial section of the marginal zone in the seventh indented annual growth ring, scale bar = 500 μm. **e** Aggregation of uniseriate and biseriate rays (arrowheads) into the multiseriate parenchyma ray (arrow) in the central region of the seventh indented annual growth ring. Cross section in the polarized light microscopy, scale bar = 100 μm. **f** Shape and size modifications of the parenchyma ray cells (arrowheads) in the marginal zone on the boundary of the seventh indented annual growth ring. Cross section in the polarized light microscopy, scale bar = 100 μm. **g** Continuing growth of hazel wood zones in the eighth annual growth ring. Aggregated multiseriate parenchyma rays (arrowheads) occur in both the marginal zones and the central regions of the hazel wood. Large disturbed zones are indicated by arrows. Tangential section in the polarized light microscopy, scale bar = 200 μm. **h** Close-up view of the aggregated parenchyma ray structure (arrows) and disturbed tracheids (arrowheads) in the eleventh annual growth ring. Tangential section, scale bar = 100 μm

that the formation of indented annual growth rings was probably caused by the intrusive growth of abnormally enlarged tracheid structures and hypertrophied parenchyma cells around the leaf traces. The pressure on the surrounding cambium initials apparently led to the suppression of the radial xylem growth around the leaf traces, thereby deflecting the orientation of the tracheids from a longitudinal direction to both longitudinal-radial and longitudinal-tangential directions. The results show that the tracheid deflection originated immediately during the first year of the onset of indentation and was dependent on the size of the disturbed zone. Alternatively, it has been reported that xylem tissues of

disturbed zones in *Pinus halepensis* showed different anatomical features and formed immediately upon the occurrence of a mechanical injury. The tissues predominantly contained traumatic resin ducts and whirled tracheids, while the emerging gaps were filled with traumatic parenchyma and large parenchyma cells in the rays (Lev-Yadun and Aloni 1991). According to Bangerter (1984) and Larson (1994), the first xylem derivatives that differentiated in wound-induced callus are often formed in a whirled arrangement. Circular elements of the xylem and the gaps filled with traumatic parenchyma were also presented in insect-produced cambial wounds (Kuroda and Shimaji 1984; Liphschitz and Mendel 1987).

A disruption of auxin flow in the cambium results in changes to both the orientation and the shape and size of the cellular elements (Aloni 2015; Larson 1994). The formation of parenchyma cells instead of tracheids probably reflects a disturbance in the axial auxin flow caused by a wound (Lev-Yadun and Aloni 1991). Yamamoto and Kozlowski (1987) and Lev-Yadun and Aloni (1991) reported that the inhibition of the basipetal transport of auxin in *Acer negundo* simultaneously reduced the local width of the wood increment and the number of vessels in the xylem, resulting in the formation of indentations in the xylem at the site of 1-N-naphthylphthalamic acid application, a polar auxin transport inhibitor.

The indentation of annual growth rings is usually caused by a local suppression of growth, where single cell elements are strongly bent, thereby resulting in the formation of depressions (Beals and Davis 1977; Rioux et al. 2003). A reduction in the formation of cell elements in the xylem may also occur during the onset of a birdseye structure formation in *Acer saccharum* (Rioux et al. 2003). Birdseye is referred to as an aberration in the normal grain pattern of maples where an indentation in the wood forms at localized points along the stem, branches, bark, and perhaps also on the roots (Bragg 2006). The abnormal development of the secondary phloem generates pressure on sensitive cambial cells, which potentially disturbs their metabolism and reduces the growth of xylem cell elements. The depth of the generated depression however was small during the onset of the indentation and changed only slightly over the next few years (Rioux et al. 2003). Contrary to the formation of birdseyes, we found that frequent malformations of both tracheids and parenchyma cells, accompanied with cell hypertrophy, immediately produced the formation of substantial lenticular depressions. The cause of indentation in birdseyes structures appears to be similar to the dimpling in some coniferous species (Bragg 1999). The formation of dimpled grains in conifers is probably due to the occurrence of resin blisters in the inner bark or the occurrence of a group of sclereids in the bark (Chafe 1969). Also, the indentations of *Fagus sylvatica* wood were caused by wedge growth of broad xylem and phloem rays (Bosshard 1974; Kučera et al. 1980), in which large sclereid structures are able to absorb the growth stresses in the phloem and shift them into the xylem tissues (Kučera et al. 1980). However, the phloem anatomy in the later developmental stages of *Picea abies* did not reveal any malformations of bark cells or the formation of abnormal structures (Nocetti and Romagnoli 2008).

Increased concentrations of lignan hydroxymatairesinol found in the disturbed zones indicate its possible role in protecting a living tree against the spread of a fungal or microbial infection at the onset of the indentation. Previous studies reported that reaction zones in *Picea abies* wood, the formation of which was induced by the fungus *Fomes annosus*, contained a significantly increased concentration of hydroxymatairesinol (up to 6% of the total dry mass fraction), whereas the sound sapwood contained negligible amounts of the lignan compounds (Hovelstad et al. 2006; Shain and Hillis 1971). At least a small part of brown stained phenolic compounds that occur in the necrotic rays of *Picea abies* wood may be related to lignans (Johansson et al. 2004). The highest concentration of hydroxymatairesinol was reported in knotwood (from 6 to 24%) because the bark and knots are especially important tissues for protecting the injured trees against a microbial attack (Kebbi-Benkeder et al. 2015; Metsämuuronen and Siren 2014).

Most hypertrophic or hypotrophic responses of the cambium appear to be caused by various pathogenic organisms such as bacteria, fungi, and insects or by specific growth disorders (Arbellay et al. 2017; Beals and Davis 1977; Nagy et al. 2005). Considering that during the early stages of P. abies annual growth ring indentation, the formation of disturbed zones occurred exclusively around leaf traces, and that within these zones, fungal hyphae were found in the surrounding tracheids along with a detected increased concentration of hydroxymatairesinol, we hypothesize that needle parenchyma tissues are potential sites for the penetration of a fungal infection into the conductive vascular tissues. Afterwards, moving through the needle vascular pathway, the fungus can attack the cambium and penetrate into the tracheids of the secondary xylem, and subsequently, cambial responses result in the formation of hazel wood.

Acknowledgments The authors thank Mrs. E. Ritch-Krč for language revision.

Funding information This work was supported by funding from the Slovak Research and Development Agency under the contract no. APVV-16-0177 (40%) and no. APVV-0744-12 (20%). In addition, this publication is the result of the project implementations: Centre of Excellence "Adaptive Forest Ecosystems," ITMS 26220120006 (20%), and Extension of the Centre of Excellence "Adaptive Forest Ecosystems," ITMS 26220120049 (20%), both of which were supported by the Research & Development Operational Programme funded by the European Regional Development Fund.

Compliance with ethical standards

Conflict of interest The authors declare that they have no conflict of interest.

References

Aloni R (2015) Ecophysiological implications of vascular differentiation and plant evolution. Trees 29:1–16

Arbellay E, Daniels LD, Mansfield SD, Chang AS (2017) Cambial injury in lodgepole pine (*Pinus contorta*): mountain pine beetle vs fire. Tree Physiol 37:1611–1621

Bangerter UM (1984) Der Verschlussmechanismus von Uingswunden am Stamm von *Larix decidua* Mill. und *Picea abies* (L.) Karst. Vierteljahrssch Naturforsch Ges Zürich 129:339–398

Beals HO, Davis TC (1977) Figure in wood: an illustrated review. Auburn University Agricultural Experiment Station Bulletin 486, Auburn, AL

Bonamini G, Uzielli L (1998) Un semplice metodo non distruttivo per riconoscere in bosco gli abeti rossi cosiddetti "di risonanza". Monti Boschi 49:50–53

Bonamini G, Chiesa V, Uzielli L (1991) Anatomical features and anisotropy in spruce wood with indented rings. Catgut Acoust Soc J 1:12–16

Bosshard HH (1974) Holzkunde 2 – Zur Biologie, Physik und Chemie des Holzes. Birkhäuser, Basel

Bragg DC (1999) The birdseye figured grain in sugar maple (*Acer saccharum*): literature review, nomenclature, and structural characteristics. Can J For Res 29:1637–1648

Bragg DC (2006) Potential contributions of figured wood to the practice of sustainable forestry. J Sustain Forest 23:67–81

Buksnowitz C, Evans R, Müller U, Teischinger A (2012) Indented rings (hazel growth) of Norway spruce reduce anisotropy of mechanical properties. Wood Sci Technol 46:1239–1246

Calvo-Flores FG, Dobado JA, Isac-García J, Martín-Martínez FJ (2015) Lignin and lignans as renewable raw materials: chemistry, technology and applications. Wiley, Chichester

Chafe SC (1969) Dimpled grain in wood. Forest Chron 45:173–179

Esau K (1965) Vascular differentiation in plants. Holt, Rinehart and Winston, New York

Fukazawa K, Ohtani J (1984) Indented rings in Sitka spruce. In: Sudō S (ed) Proceedings of Pacific regional wood anatomy conference. Forestry and Forest Products Research Institute, Tsukuba, pp 28–30

Gričar J, Prislan P, Gryc V, Vavrčík H, de Luis M, Čufar K (2014) Plastic and locally adapted phenology in cambial seasonality and production of xylem and phloem cells in *Picea abies* from temperate environments. Tree Physiol 34:869–881

Grosser D (1986) On the occurrence of trabeculae with special consideration of diseased trees. IAWA Bull 7:319–341

Hovelstad H, Leirset I, Oyaas K, Fiksdahl A (2006) Screening analyses of pinosylvin stilbenes, resin acids and lignans in Norwegian conifers. Molecules 11:103–114

Imamura Y (1981) Anatomical characteristics of decorative shugi logs in Japanese wooden structure. In: Hillis WE (ed) Proceedings of the 17th IUFRO Congress, Division 5. Kyoto, Japan, pp 1–5

Johansson SM, Lundgren LN, Asiegbu FO (2004) Initial reactions in sapwood of Norway spruce and Scots pine after wounding and infection by *Heterobasidion parviporum* and *H. annosum*. For Pathol 34:197–210

Kebbi-Benkeder Z, Colin F, Dumarçay S, Gérardin P (2015) Quantification and characterization of knotwood extractives of 12 European softwood and hardwood species. Ann For Sci 72:277–284

Kučera L, Bosshard HH, Katz E (1980) Über den Keilwuchs und den welligen Jahrringverlauf in Buche (*Fagus sylvatica* L.). Holz Roh Werkst 38:161–168

Kuroda K, Shimaji K (1984) Wound effects on xylem cell differentiation in a conifer. IAWA Bull 5:295–305

Larson PR (1994) The vascular cambium—development and structure, 1st edn. Springer-Verlag, Berlin

Lev-Yadun S, Aloni R (1991) An experimental method of inducing 'hazel' wood in *Pinus halepensis* (*Pinaceae*). IAWA Bull 12:445–451

Liphschitz N, Mendel Z (1987) Histological studies of *Pinus halepensis* stem xylem affected by *Matsucoccus josephi* (Homoptera: Margarodidae). IAWA Bull 8:369–376

Metsämuuronen S, Siren H (2014) Antibacterial compounds in predominant trees in Finland: review. J Bioprocess Biotech 4:167–180

Nagy NE, Krokene P, Solheim H (2005) Anatomical-based defense responses of Scots pine (*Pinus sylvestris*) stems to two fungal pathogens. Tree Physiol 26:159–167

Nelson T, Dengler N (1997) Leaf vascular pattern formation. Plant Cell 9:1121–1135

Nocetti M, Romagnoli M (2008) Seasonal cambial activity of spruce (*Picea abies* Karst.) with indented rings in the Paneveggio forest (Trento, Italy). Acta Biol Cracov Ser Bot 50:27–34

Ohtani J, Fukazawa K, Fukumorita T (1987) SEM observations on indented rings. IAWA Bull 8:113–124

Račko V, Mišíková O, Čunderlík I, Seman B (2016) Indentation of juvenile annual growth rings and their impact on morphology of wood cells. Key Eng Mater 688:175–181

Rioux D, Yamada T, Simard M, Lessard G, Rheault FJ, Blouin D (2003) Contribution to the fine anatomy and histochemistry of birdseye sugar maple. Can J For Res 33:946–958

Schneider L, Gärtner H (2013) The advantage of using a starch based non–Newtonian fluid to prepare micro sections. Dendrochronologia 31:175–178

Schultze DG, Gotze H (1986) Abnormal wood structure: 'hazel grain' and wavy grain. Wood Res 111:1–10

Shain L, Hillis WE (1971) Phenolic extractives in Norway spruce and their effect on *Fumes annosus*. Phytopathology 61:841–845

Tsoumis G (1968) Wood as raw material: source, structure, chemical composition, growth, degradation and identification. Pergamon Press, London

Willför S, Hemming J, Reunanen M, Eckerman C, Holmbom B (2003) Lignans and lipophilic extractives in Norway spruce knots and stemwood. Holzforschung 57:27–36

Yamamoto F, Kozlowski TT (1987) Regulation by auxin and ethylene of responses of *Acer negundo* seedlings to flooding of soil. Environ Exp Bot 27:329–340

Yaman B (2007) Anatomy of Lebanon cedar (*Cedrus libani* A. Rich.) wood with indented growth rings. Acta Biol Cracov Ser Bot 49:19–23

Ziegler H, Mertz W (1961) Der "Hasel" wuchs Über Beziehungen zwischen unregelmäßigem Dickenwachstum und Markstrahlverteilung. Holz Roh Werkst 19:1–8